AMERICAN UNIVERSITY OF BEIRUT

# TOWARDS A 3D-PRINTED IOT ELECTRONIC NOSE FOR MULTIPURPOSE AROMATIC DISCRIMINATION: AN OPEN SOURCE, LOW COST, AND PORTABLE SOLUTION TESTED ON WINE

by
AHMAD FARAJ KHATTAB

A thesis
submitted in partial fulfillment of the requirements
for the degree of Master of Engineering
to the Department of Electrical and Computer Engineering
of the Faculty of Engineering
at the American University of Beirut

Beirut, Lebanon
April 2019

AMERICAN UNIVERSITY OF BEIRUT

# TOWARDS A 3D-PRINTED IOT ELECTRONIC NOSE FOR MULTIPURPOSE AROMATIC DISCRIMINATION: AN OPEN SOURCE, LOW COST, AND PORTABLE SOLUTION TESTED ON WINE

by

AHMAD FARAJ KHATTAB

Approved by:

[Signature] _____

[Dr. Mariette Awad, Associate Professor]
[Department of Electrical and Computer Engineering]
Advisor

[Signature] _____

[Rabih Jabr, Professor]
[Department of Electrical and Computer Engineering]
Member of Committee

[Signature] _____

[Imad Toufeili, Professor]
[Department of Nutrition and Food Sciences]
Member of Committee

Date of thesis/dissertation defense: [April 25, 2019]

# AMERICAN UNIVERSITY OF BEIRUT

# THESIS, DISSERTATION, PROJECT RELEASE FORM

Student Name: Khattab (Last) Ahmad (First) Faraj (Middle)

● Master's Thesis ○ Master's Project ○ Doctoral Dissertation

☐ I authorize the American University of Beirut to: (a) reproduce hard or electronic copies of my thesis, dissertation, or project; (b) include such copies in the archives and digital repositories of the University; and (c) make freely available such copies to third parties for research or educational purposes.

☒ I authorize the American University of Beirut, to: (a) reproduce hard or electronic copies of it; (b) include such copies in the archives and digital repositories of the University; and (c) make freely available such copies to third parties for research or educational purposes after:

One ---- year from the date of submission of my thesis, dissertation, or project.
Two ---- years from the date of submission of my thesis, dissertation, or project.
Three --X-- years from the date of submission of my thesis, dissertation, or project.

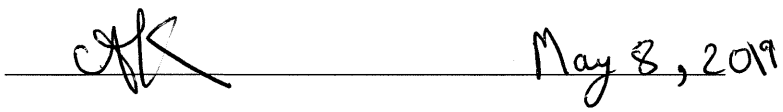

May 8, 2019

Signature Date

# ACKNOWLEDGMENTS

I want to thank the following people for their support in completing this thesis:

Marwa El Ghali, for never failing to hold down the fort, allowing me to dedicate the time needed to this thesis,

My Secret Santa this year, for helping supply some of the wine for testing,

Marwa Itani, for her help in the lab, as well as all other lab instructors along the way,

Dr. Imad Toufeili, for his support and guidance in the lab and the experiments,

My advisor, Dr. Mariette Awad, for her constant guidance and her patience,

And finally, and most importantly, my family, for being the shelter I can go to whenever I lose my way.

# AN ABSTRACT OF THE THESIS OF

Ahmad Faraj Khattab for Master of Engineering
Major: Electrical and Computer Engineering

Title: Towards a 3D-Printed IoT Electronic Nose for Multipurpose Aromatic Discrimination: An Open Source, Low Cost, and Portable Solution Tested on Wine

The sense of smell or olfaction is a primary human sensory system and perhaps the most evocative of the five senses eliciting strong emotional and cognitive responses of both attraction and repulsion. The human olfactory system can detect more than 10000 odors and can discern up to 5000 of them. The human ability to discriminate and detect different odors is however very limited, highly subjective and prone to fatigue. As a result, there have been increasingly many attempts at mimicking the sense of smell in what has now been known as an electronic nose or an e-nose.

In the biological olfactory system, the neural network plays the crucial role of coding, processing, and classifying the different odors based on the neural signals received from the olfactory receptors' interaction with odorants. Similarly, in an e-nose, an array of non-specific chemical sensors reacts to the aerosols, altering them to varying degrees, which gives rise to electrical signals that are registered by the instrument. Various pattern recognition methods can then be employed to discriminate the unknown odors into predefined fingerprints. This potential to discern different odors at a significantly lower cost and time has fueled the research of utilization of e-noses in many fields. However, commercialized e-noses are still bulky, expensive, and offer a closed system that is very specific in terms of the sensor configuration and the aerosols that can be monitored, targeting niche markets with proprietary software.

This thesis presents a novel portable, versatile, 3D Printed IoT connected e-nose, the advantages of which consist of its open source nature, ease of reproducibility and mass employability for a cost of around $200. The e-nose was tested in a wine classification exercise where different machine learning approaches were used, and the best one yielded a 99% aroma prediction accuracy showing the potential of the proposed e-nose to service mass markets and compete to a large extent with commercial units.

# CONTENTS

# ILLUSTRATIONS

# TABLES

# CHAPTER I

# INTRODUCTION

The sense of smell or olfaction is a primary human sensory system and perhaps the most evocative of the five senses eliciting strong emotional and cognitive responses of both attraction and repulsion. Olfaction's primary role is in regulating food intake and contribution of up to 75% to the perception of flavor. It also serves a protective function against possible toxic materials or irritants. The human olfactory system can detect more than 10000 odors and can discern up to 5000 of them [1, 2]. The ability to detect the presence of certain aerosols has proven to be of great potential and of great use in a wide range of fields, from detecting bombs, spoilage of food, pollutants, to diagnosing various diseases such as diabetes and cancer. The human ability to discriminate and detect different odors is however very limited, highly subjective and prone to fatigue. Thus far, societies have relied on dogs to detect odors in different domains ranging anywhere from safety and security to health and quality control. However, training canines to detect certain odors is greatly restricted by the cost of training a dog which also has a short life expectancy and the limitation of the olfactory system of the dog itself. As a result, there has been increasingly many attempts at mimicking the sense of smell in what has now been known as an electronic nose or an e-nose [3, 4]. While a nose leads to odor identification which is subjective and highly aesthetic, an e-nose is an instrument with an array of non-specific chemical sensors which lead to odor discrimination as shown in Fig. 1. In the biological olfactory system,

the neural network plays the crucial role of coding, processing, and classifying the different odors based on the neural signals received from the olfactory receptors' interaction with odorants. Similarly, in an e-nose, an array of non-specific chemical sensors react to the aerosols, altering them to varying degrees, which gives rise to electrical signals that are registered by the instrument [5]. Since the chemical gas sensors are different, a multivariate response with broad and partially overlapping selectivity to each sample aerosol will be obtained. The result is a unique pattern that characterizes the aerosol. As such an aerosol which can be odorous or odorless is classified without insight to the nature or constituents of the odor. Pattern-recognition algorithms would allow for the classification of the different aerosols based on their fingerprint response to the chemical sensors [6-8].

This potential to discern different odors at significantly lower cost and time has fueled the research of utilizing e-noses in many fields from food industry[9, 10], safety [11, 12], disease and cancer detection [13, 14], to monitoring environmental pollution on earth as well as space stations [15-18].

However, one of the main restrictions of the technology so far has been validation [19]. The successful implementation of the e-nose in various applications requires a large number of well-characterized samples to carry out an appropriate training. The way to solve this problem is to construct international databases. Commercialized e-noses might offer solid methodology for standardized data collection, and several groups are currently working on the construction of databases that will help to improve the quality of validations [20].

However, commercialized e-noses are still bulky, expensive, and offer a closed system that is very specific in terms of the sensor configuration and the aerosols that can be monitored. This restricts the widespread use, validation and crucial data collection for specific applications [4, 7, 9, 10]. The reliance of successful e-nose applications on using machine learning algorithms imposes the need for abundance of data and that requires cheap, easy-to-use tools that are uniform across data collectors.

To this end, this thesis presents the development of an IoT open source version of a multipurpose, customizable, low-cost, portable, 3D-printed, connected e-nose. While extensive research is going into development of low-cost and compact devices, to the best of our knowledge, this is the first e-nose of open source nature. This design was manufactured and customized with basic CNC, 3D printer and electronic knowledge at a very low cost (around 200$) making it highly accessible to educational institutions, universities and the scientific research community. In the scope of this work, we tested the e-nose in a classification exercise for different wine types both local and international.

The remainder of this thesis is organized as follows. Chapter 2 reviews the current state-of-the-art e-noses, both commercial and those proposed by other research groups. Chapter 3 describes the proposed e-nose hardware, while chapters 4 and 5 discuss its workflow and enclosure specifications respectively. Chapter 6 presents a case study of the proposed e-nose for classification of different wine types, with the set of results summarized in chapter 7. Finally, chapter 8 discusses conclusions of this project and proposed future work.

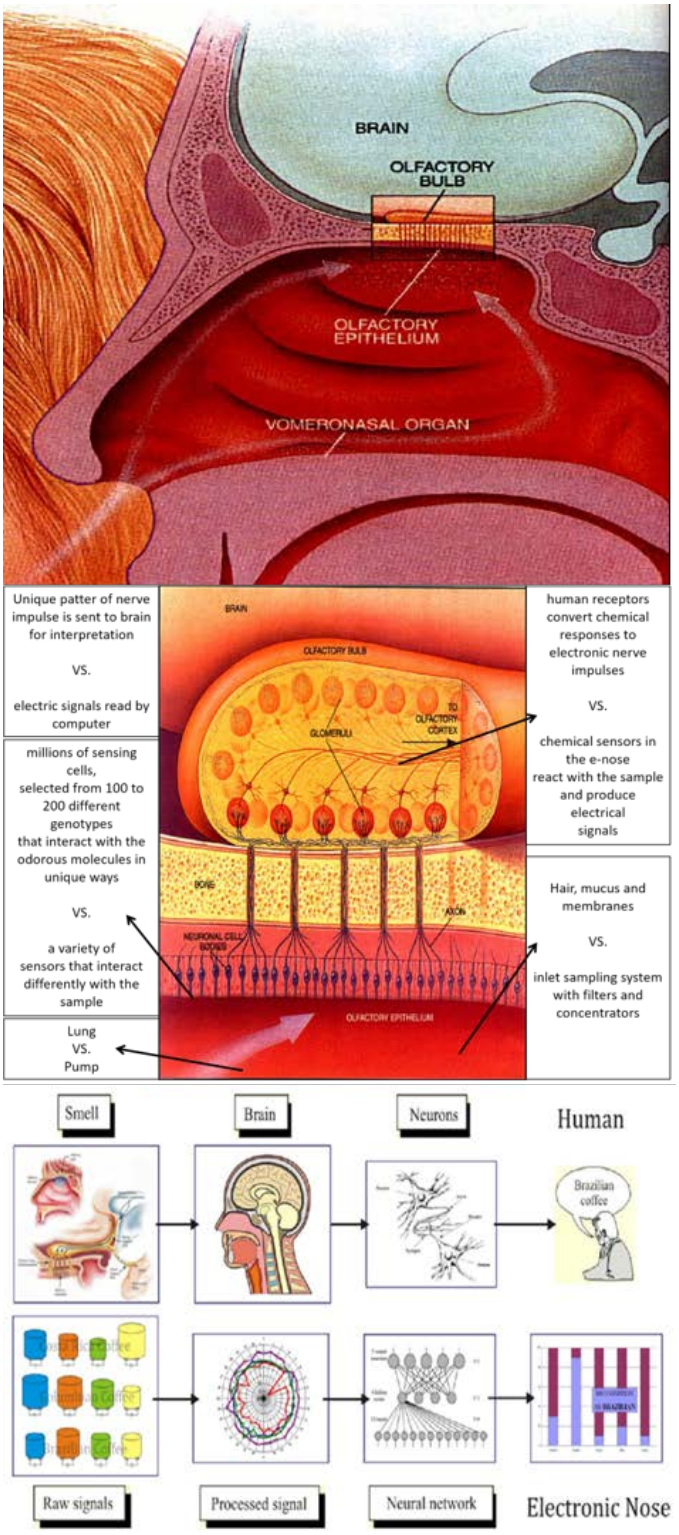


Fig. 1: From a Nose to an E-Nose [5], edited from [1]

# CHAPTER II
# RELATED WORK

E-noses can offer a viable solution for detection of aerosols and odors by allowing for real-time continuous measurements. However, most e-nose technologies have been bulky or at best semi-portable, while lacking reconfigurable and accessible design [21]. Although some commercial e-noses have achieved good portability with a hefty price tag, like the PEN3 at 19,800 Euros (2019 quotation) [21], most e-nose solutions have employed desktop stationary stations [6]. The high cost is due to the sensors employed, which are often very expensive and selective, limiting the range of usage of a certain type of e-nose [4]. The current market leader in electronic noses is the French company Alpha Mos, which offers high-end, expensive, robust stationary laboratory e-noses. Other companies, like Scensive Ltd and Smiths Detection, offer somewhat cheaper and more portable versions of e-noses, which are frequently utilized in academic literature. These devices are intended to be used as laboratory instruments and are based on conducting polymer arrays. Some examples include the ppbRAE Plus with listed price of $6,215 and the portable Cyranose320 with listed price of $7,995, according to a 2014 sale quote from (www.sensigent.com) [21]. Another company, Electronic Sensor Technology Inc., offers their “zNose” model which ranges from $30,000 to $45,000 according to 2019 quotation.

Due to the continuous advances in gas sensor technology, research groups have given rise to exceptions that address these limitations [22]. MOSES II, developed by GSG group, allows for multiple configurable sensor technologies in one device. The

aim, however, was optimized for accuracy and precision over portability. It is a heavy stationary unit with Metal Oxide and Quartz microbalance sensors and unsuitable for mobile applications [23]. Other e-noses that were developed, like the X-AM 7000 by Dräger [22], exhibited excellent portability. However, the device was application-specific for detection of aerosols for human safety at industrial plants, which is a limitation of the scope. Likewise, there are similar e-noses published in research developed by universities and research facilities interested in e-nose technology in one specific type of application [24-26]. Another drawback facing e-nose technology is the direction of many universities to design their own from the ground up to suit their needs and their budgets avoiding utilizing a commercial costly e-nose. This greatly restricts reproducibility and validation when the design is halted at a make-shift prototype stage or kept proprietary to be commercialized later for a high price tag [27-32]. As such, the work presented by our thesis still acquires a unique niche and special interest for the scientific community to utilize a simple yet innovative technology.

# CHAPTER III

# PROPOSED IOT HARDWARE

The intended target of the proposed e-nose is not to compete with the existing high-end laboratory-specific market, but to address mass markets. The target is to have a low-cost, battery-operated, IoT e-nose that can be created with ease for eventually multiple applications. The ability to produce an e-nose with consistent unit-to-unit properties enables calibration on one unit, and application to all units' methods, which is crucial to solving e-nose's challenge of validation [33].

To maintain a low-cost product, the suggested e-nose implements Metal Oxide Sensors (MOS) which are among the cheapest, most commercially-available gas sensors. The basic concept of operation of these sensors is based on a sensor element and a heater element. Metal oxides on the sensor element reach high temperatures due to the heater, at which point they behave as semiconductors and induce redox reactions with the surrounding aerosols at their surfaces in presence of ambient oxygen. The degree of reactivity is determined by the metal oxide / catalyst combination, the surrounding aerosols, and the temperature. The resistance of the MOS changes as a result and can be measured by the e-nose as voltage variation. These sensors are robust with broad reactivity to a wide range of aerosols, which is perfect for usage in e-nose technology, albeit their sensitivity to temperature and moisture [34-36].

To increase the range of its utility as a multipurpose device, the suggested e-nose would have replaceable sensors that can be exchanged to suit the intended purpose.

The e-nose would have sockets that fit different models of gas sensors, allowing detection of aerosols for different applications. The suggested e-nose would cut the design stage and allow interested parties to jump directly into testing, by choosing whichever sensors they wish to utilize. After reviewing the most important metal oxide gas sensor models on the market, the most popular were chosen for the design, which are the Figaro line of MOS, and their corresponding sockets Figaro's TGS8xx and TGS2xxx [26, 34, 37, 38]. For the test case, eight commercially-available Figaro gas sensors that cover a large range of smells were chosen.

The e-nose classification workflow consisted of training and testing phases. A training stage introduces the e-nose to specific aerosols and assigns the known class to the response from the sensors. The testing stage introduces new samples to the e-nose and tests for successful classification.

**A. Main PCB**

The main PCB holds the e-nose's microcontroller, Bluetooth module, and the sensors' variable resistors. The board was printed on a regular commercial double-sided board. The board acts as a breakout for the pins of the microcontroller. We added redundant connectors for future possibility of expanding the components of the e-nose including a secondary pump, a valve control, as well as digital inputs/outputs.

### *1. Arduino Pro Mini*

The e-nose uses an Arduino Pro Mini as its microcontroller. The wildly popular development board, especially in educational institutions, bridges the gap between flexible prototyping and permanent set-ups, allowing for both rapid testing and fixed installations in a project. The 5 volts version was selected as opposed to 3.3 volts to avoid the need for unnecessary voltage regulators. The board comes with headers that allow it to be mounted into PCBs directly. An FTDI cable or FTDI to USB board can be used to communicate and program the device with ease while maintaining a minimal size. An open source Arduino IDE with plenty of community support is used to program the controller. The small board packs up to 14 digital inputs/outputs including 6 PWM outputs and 6 analog inputs, which offers plenty of flexibility to expand our sensory input and functionality further [39]. The pinout can be seen in Fig. 2.

### *2. Bluetooth Mate*

The Bluetooth module from Sparkfun offers a simple method to add connectivity to the e-nose. It can both send and receive data and can be readily connected to the Microcontroller serially and with 5 volts to power up [40].

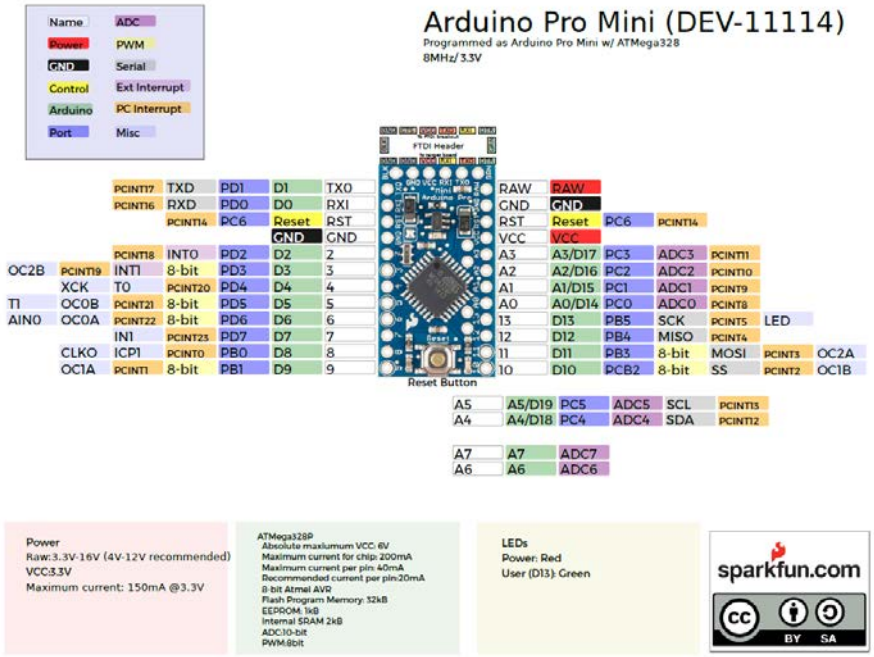


Fig. 2: Arduino Pro Mini Pinout [40]

### *3. Multi-Turn Trim Potentiometers*

The variable resistors offer control over the sensitivity of the Figaro Gas sensors and the flexibility to adjust according to the application or aerosols of interest. They are ergonomically placed directly underneath a magnetic cover, which exposes them when removed for ease of access as shown in Fig. 3.


Fig. 3: A magnetic cover gives access to the variable resistors controlling the sensors

**B. Sensors PCB**

The sensors' PCB is the second main circuit of the E-nose. It is also the simplest, so we printed it on single-sided boards. It is made up of 8 sockets that are evenly distributed between 4 pins - marked as S0, S1, S6, S7 in Fig. 4, and 4 pin formats marked as S2, S3, S4, S5. These can house the two main types of MOS. The arrangement of the sockets is crucial to eliminate sensor bias when the flow of aerosols is first introduced to the sensor chamber.

As shown in Fig. 4, the sockets where arranged with equal distance from the center where the aerosol is administered. The optional noticeable edge to the otherwise

circular board allows for intuitive correct orientation placement when assembling the device, as it can only be fitted in one way. To allow for modifications on the number of sockets and their type, we purposefully developed the sensors' PCB separately. It interfaces with the main PCB via connecting wires. The PCBs can be replicated using the files generated from the free version of EAGLE, PCB Design Software, from Autodesk.

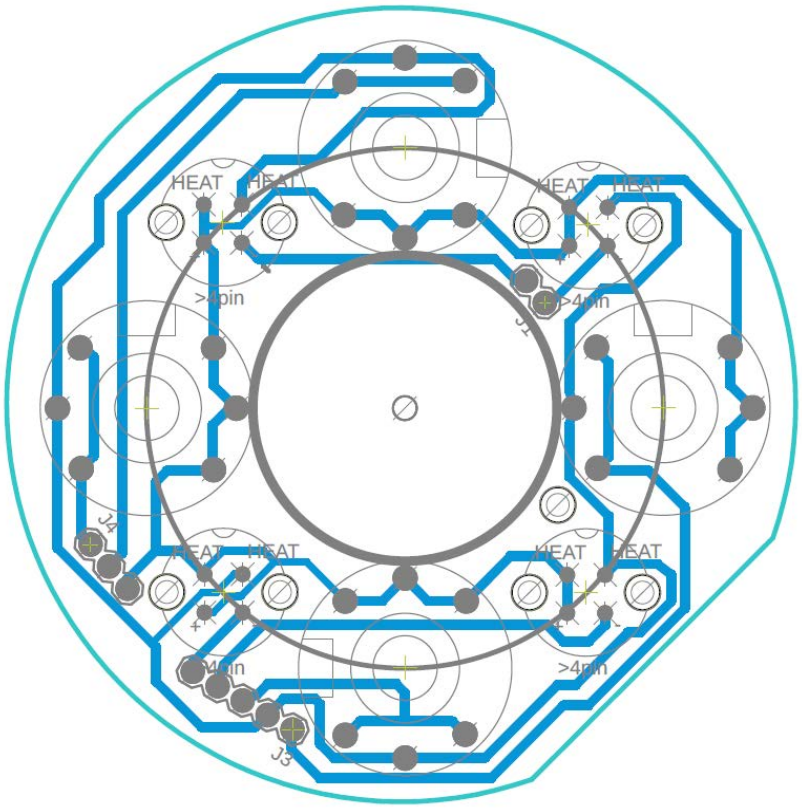


Fig. 4: An eagle file schematic of the sensors' PCB

## C. Others

### *1. Power Source*

A battery pack from a disassembled Power bank (Anker Portable Charger Power Core 20100 mAh) powers the e-nose. This simplifies the manufacturing further as the charging circuitry can be directly incorporated into the design, allowing for recharging by USB.

### *2. Pump*

A simple 6V DC Mini Air Pump is used to allow the e-nose to “sniff” in the aerosols. For this purpose, we’ve utilized the Mini Air Pump Motor. It’s made of metal and plastic, has a 6V operating range voltage, and allows for 0.5L of air flow.

### *3. 12-Volts Micro Solenoid Valve*

A single 12V micro solenoid valve, which can be controlled digitally via the microcontroller, was used. This is crucial for the different working modes of the e-nose. It is placed at the output to trap or release the aerosols extracted by the pump or injected into the sensors’ chamber.

### *4. 5V-12V Step-up Voltage Regulator*

A voltage regulator was utilized to operate the 12V Solenoid Valve. This added complexity can be avoided if a suitable 5 volts micro solenoid valve was found in the local market.

### *5. 3 Configurable Control Buttons*

The Arduino microcontroller supports 6 configurable control buttons. Three momentary push buttons were added to the interface of the e-nose enclosure to control different functions. The In this setup they corresponded to Cleaning Button, Auto Sampling Button, and Continuous Sampling Button. The cleaning button initiates the cleaning mode necessary to clear the aerosol chamber from any contaminants or aerosol residue from measurements. The sampling button initiates a timed sampling mode which can be configured to last for a set duration allowing for precise operation of the pump and withdrawal of a specific volume of aerosol headspace. The continuous sampling button allows for continuous sampling and is mainly used for quick testing of aerosol headspace with no time restrictions.

### *6. One-Way Valve*

This passive one-way valve was used to prevent the back flow of collected sample aerosols once the pump is shut off after sampling. It is placed at the inlet. This and all other parts mentioned can be seen in Fig. 8 below, as part of the dissected schematic of the proposed e-nose.

# CHAPTER IV

# PROPOSED MODE OF OPERATION

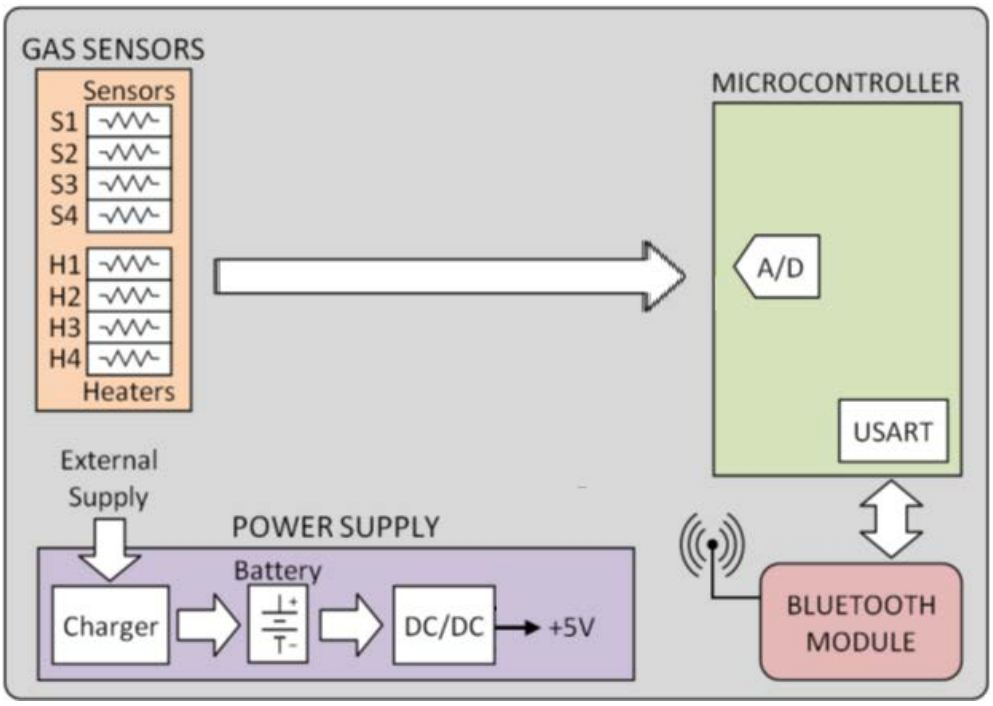


Fig. 5: A typical e-nose workflow

The e-nose's mode of operation is dictated by the software that is uploaded to its microcontroller. In principle, e-noses share a similar workflow as shown in Fig. 5. The microcontroller reads the responses registered by the gas sensors as a voltage measured at the output of the voltage divider, and then either saves them locally or transmits them to a receiving medium. In our suggested e-nose, an Arduino microcontroller transmits the data collected via Bluetooth to a visualizing tool deployed on a PC. The code that runs the setup can also be generated and applied using the open

source Arduino IDE. The e-nose's workflow operates according to the following steps as shown in Fig. 6:

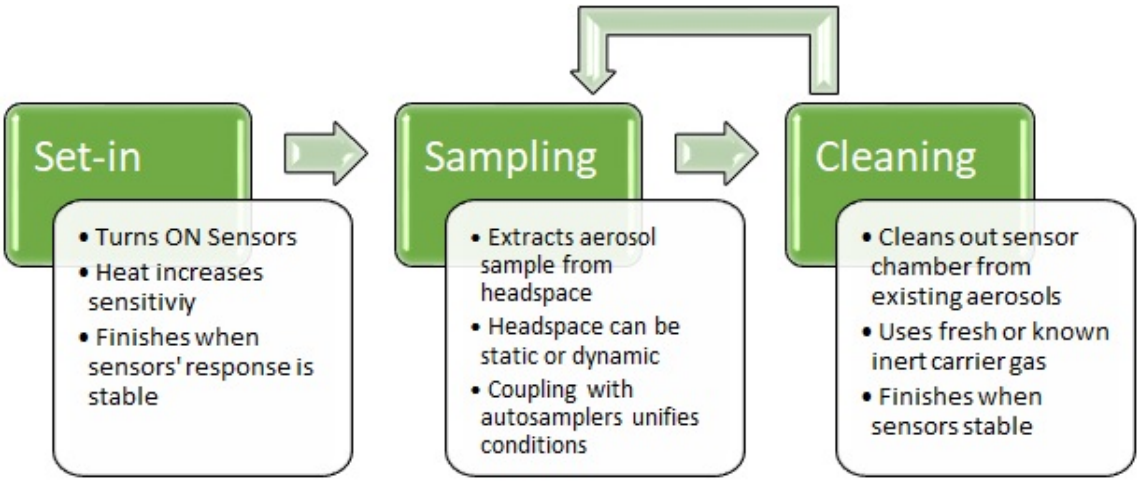


Fig. 6: A typical e-nose steps of operation

**A. Set-In Phase**

Considered as the initial state of the e-nose, it must be carried out to completion before any aromatic sampling starts. In this state, the e-nose is turned on and sensors become active. The sensors usually require some time to achieve their optimal working conditions. In the case of MOS, this state is usually referred to as the Burn-in or Set-in phase. The heater components of the MOS increase in temperature, which increases the sensitivity of the gas sensors. The end of this phase is usually signaled by the stabilization of the recorded responses from the e-nose.

**B. Sampling Phase**

The methodology followed when sampling in e-noses depends largely on the type of sample. In simple mixtures of single gases or well-known combination of gases, it suffices to prepare the aerosols by mixing the gases from predefined gas bottles. A mass flow controller is used to get the required concentrations and percentages of each. However, in complex mixtures like food odors, the aerosol sample in question is to be collected from the headspace of sealed vials in which the sample is placed [41-43]. A headspace is simply the contained aerosol medium which the sample would have released odors into. If the sample is allowed to sit in the sealed vial for some time, it continuously releases vapors into the medium until equilibrium or saturation occurs. The speed at which this release occurs, and the volume of aerosols released depends on the surface area, the sample concentration, its volatility and the sample temperature.

There are multiple schemes for sample collection: two of the most common are referred to as dynamic headspace technique and static headspace technique. In the dynamic headspace technique, an inert carrier gas flushes the aerosols from inside the vial and into the e-nose. This continuous sweeping over the liquid phase of the sample keeps the concentration of aerosols in question very low in the sealed vial, which allows for continuous release of more sample aerosols as equilibrium or saturation is never achieved. In static headspace technique, the headspace in a sealed vial is extracted by a syringe or pump suction and injected into the sensor chamber of the e-nose [28, 42, 43].

In both schemes, an external auto-sampler like the (Hs 850 CE Instruments) can be used [27, 44]. This device automates the sample collection, increases the

reproducibility of measurement due to its automated nature, and often improves upon the accuracy of the results. It consists of a belt-like rotary that samples from different vials sequentially or in parallel. The conditions of the extracted aerosol samples can be controlled by exposing them to heat or reducing humidity etc. As such, each sample is extracted with the same characteristics of speed, volume, and most importantly similar temperature and humidity conditions.

The suggested e-nose is compatible with both techniques and can also be coupled with an autosampler. Although the e-nose has a built-in pump, it can be readily bypassed and the autosampler in this case would inject the sample aerosols instead of them being “sniffed” or sucked in.

**C. Cleaning Phase**

This is the final phase in the e-nose workflow which allows, upon completion, for another sampling. Fresh or known inert carrier gas is now injected or extracted into the sensors’ chamber. It is intended to purge and clean the sensors of any aerosols that are present from the previous sampling. The end of this phase is usually signaled by the stabilization of the recorded responses from the e-nose. The time required here varies depending on the nature of the aerosols from the previous samples, and the sensors’ drift might be noticeable afterwards.

# CHAPTER V

# PROPOSED ENCLOSURE

To allow ease of reproduction and assembly, the e-nose's enclosure was manufactured in LEGO-like modules. The enclosure can readily be assembled or disassembled partially or fully with a single standard screw driver. This gives users access to any part of the inside of the e-nose to connect the circuitry during assembly or for troubleshooting. As a result, multiple materials were used to fit each module. Three main materials were used: PLA Plastic, Polyamide, and Plexiglas. All three manufacturing procedures were done using tools and equipment typically found in universities and laboratories. The entire enclosure can be replicated by using the open source design directly. One important feature that must be done manually is securing the seal of the sensors' chamber.

## A. Polyamide Parts

The sensors' chamber, which is composed of the top chamber and top lid as shown in Fig. 7, are indeed the most crucial part of the e-nose. They will be exposed to the most amount of heat from the sensors' operation as well as integration with the incoming aerosol samples. As such, they should exhibit inert properties and high tolerance to heat. For that reason, they were made from a material like Teflon but at a much lower price tag. Both were manufactured using the Roland 540 CNC machine operating with 3 axes. Originally, 2 single blocks of white polyamide were fitted to the

CNC. Files are exported as STL and processed with Vectric Aspire. The air opening was manually drilled with a 3mm drill bit.

**B. PLA Plastic Parts**

These parts have the most intricate design in the e-nose. As such, it was necessary to use 3D printing to manufacture them as they would otherwise prove hard to do using a normal CNC machine. The top bracket, back panel, and side arcs, shown in Fig. 7, were manufactured using the Dreamer Flashforge 3D printer. The filament used is a black PLA. Files are exported as STL and processed with Dreamer software. The machine settings for the above prints are: 85 degrees Celsius for the bed temperature, 220 degrees Celsius extruder temperature, medium resolution prints, 25% infill hexagon-shaped supports and raft are also added. After finishing the prints, we fitted 3mm threaded inserts to the holes by heating them with a hot air gun. Two magnets were added to the side arcs to allow for ease of removal of the cover and access to the multi-turn trim potentiometers.

**C. Plexiglass Parts**

Because these parts have a simple form, it was more accurate and economical to manufacture them using CNC machine. The front panel, side panels, front lid, and bottom lid, shown in Fig. 7, were manufactured using a 100W laser cutting machine. 4mm black opaque Plexiglas sheets were used. We exported the files as DXF and processed them with AutoLaser software. The front lid was then treated with the CNC


Fig. 7a: A 3D rendering of the proposed e-nose


Fig. 7b: Proposed e-nose

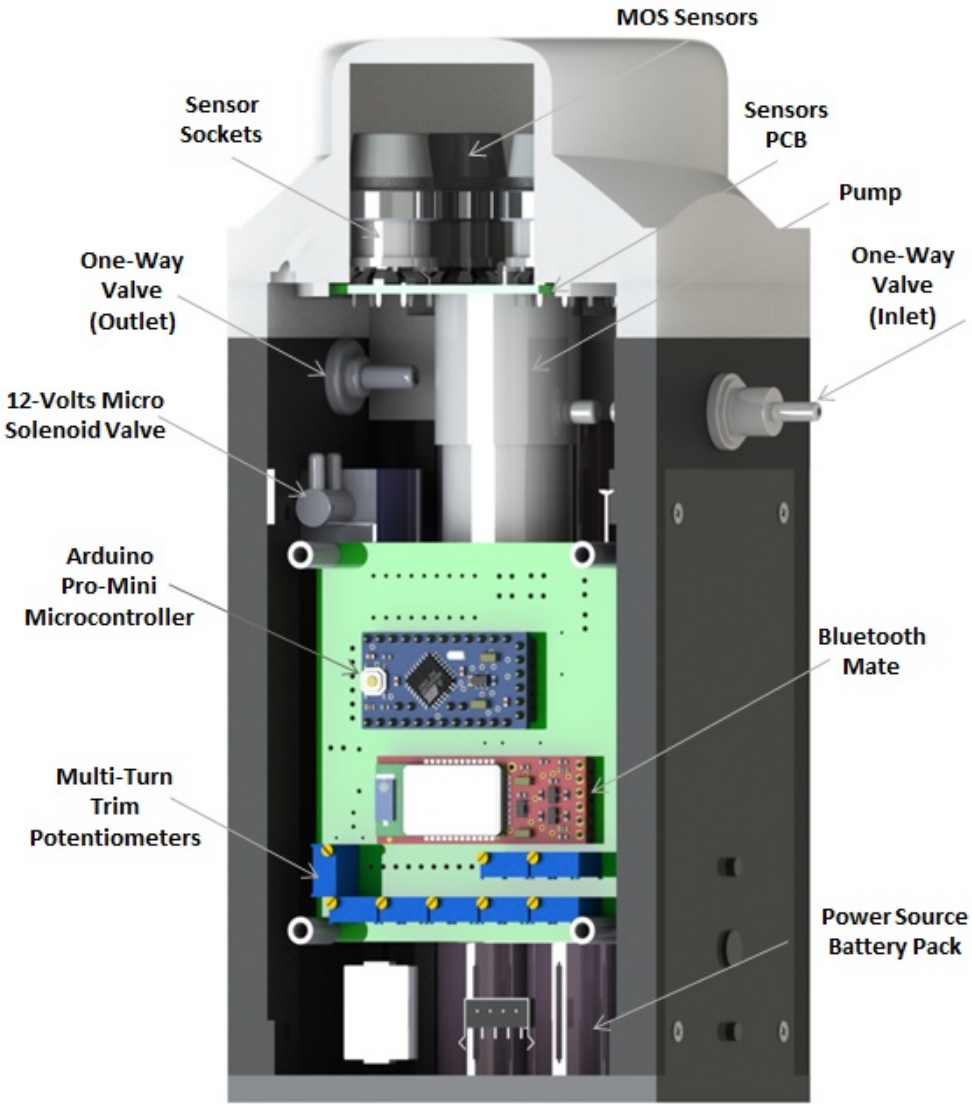


Fig. 8: A 3D cross-section rendering of the proposed e-nose

to engrave the logo, numbers, and place the magnet placeholders. After cutting all parts, we manually drilled the chambers with an electric drill. Two magnets were added to the front lid. White paint was applied to highlight the engraved text. The lid was treated with the CNC to give space for the battery cables. Similarly, the left side of the Plexiglas was treated with the CNC to add room for the micro solenoid valve to rest.

**D. Sensors' Chamber Seal**

To favor reproducibility by eliminating variables that affect the sensors' behavior, namely humidity and temperature, the top chamber and top lid were both sealed with liquid rubber to prevent air from escaping outside of the chamber. The rubber seal was poured into the groves between the two: it was left 24 hours in warm room temperature conditions for a better overall performance and was later treated for 8 hours in 65 degrees Celsius atmospheric temperature. Upon its settling, the liquid rubber hardened and acted as a customized O-ring. The liquid rubber is commercially available with simple instructions to apply, resembling preparation of your mainstream Gelatin or Jell-O. Finally, we applied a disposable layer of self-adhesive silicon wherever measurements were due to ensure full seal of the sensors' chamber.

# CHAPTER VI

# CASE STUDY EXPERIMENTATION

To test the proposed e-nose, we performed a classification exercise of different types of wines from various local and international brands. Wine has an intrinsic aroma that is considered a telltale sign of its quality and type. The aerosols generated by wine are a complex mixture of volatile organic compounds that each contribute in different capacities to the odor and smell detected [45]. Minute changes in these aerosols or their concentrations might alter the perceived aroma characteristics, and that is usually reflected in the price paid for the wine [44]. The quality of wines has been long evaluated by an expert sensory panel: a group of trained humans who rely on their olfactory senses to differentiate and discern the quality of wines. However, securing and training a sensory panel is both costly and time-consuming. It is also susceptible to human bias and fatigue [46]. Other wine evaluation techniques involved laboratory analysis of the chemistry of the wines by analytical instruments such as gas chromatography and mass spectrometry. These tests give an understanding of the molecules, which might be volatile, and the aerosols released by wine, but fail to capture the subjective nature of the odor that ends up being perceived [45]. They are also lacking in simplicity and tend to require significant preparation and analysis time, restricting usability to expert operators [27].

However, new approaches that combine data measured from multiple instruments, such as gas or NMR chromatography, mass spectrometry, FTIR spectra,

promise a more accurate evaluation. This holistic approach to measurements, inspired by the biological olfactory system, looks at the global information collected about the sample as opposed to its individual components or characteristics [47].

Similarly, the e-nose's array of some specific, cross-sensitive sensors, combined with machine learning algorithms, offer multiple data inputs that give rise to an identifiable, unique fingerprint for the wine's aroma. The simplicity of utilizing a single device for odor classification has made e-noses very popular in the analysis of wines in many applications including quality control, age monitoring, or the detection of adulterants [46]. Table 1 summarizes some of the applications and research on e-nose usage in wine study and classification.

| Application/Case Study | Samples | E-nose Technology | Remarks |
|---|---|---|---|
| Use of synthetic wines to calibrate e-nose for natural wines [48] | three varying characteristic compounds in wines | HS-MS, or headspace and mass spectrometer E-nose which is a composed of two laboratory stationary equipment | reduction of errors when calibrating with synthetic wines over time |
| Identification of typical wine aromas [49] | a total of 16 aromas | E-nose used has been home fabricated. The sensor array was prepared by 16 thin film tin oxide sensors. The e-nose is coupled with a headspace sampling setup. | discriminates the different aromatic signatures of varying wine flavors |
| Differentiation and classification according to origin, variety and ageing [50] | 3 Spanish wines with aged and fresh variant of each type | HS-MS e-nose | discriminates the according to origin and variety was more successful than aging |
| Classification of four types of Barbera wines and produced in different in enclosed geographical areas [51] | Four types having different origin | PEN2 commercial e-nose of 10 metal oxide | 98.1% correct prediction coupled with data from Electronic Tongue |

Table 1: Different e-nose applications and research in wine study and classification [48-51]

## A. Proposed Experimentation Strategy

To prepare for our wine classification test case, a couple of arrangements were considered:

### *1. Sensors Selection*

MOS have been successfully frequently used in e-noses in wine-related applications for classification of flavors, region, aging and others in spite of their high sensitivity to water [9, 43, 46]. Similarly, this setup used 4 Figaro TGS26XX (with XX = 00,02,12,20) and 4 Figaro TGS8XX (with XX = 16,26,23,32) obtained from Figaro Engineering, Inc. [52]. These sensors are sensitive towards a wide spectrum of gas types with overlapping sensitivities. Table 2 lists the target gases of the 8 MOS provided by the manufacturer.

| Sensor Name | Target Gases |
|---|---|
| TGS816 | Combustible Gases |
| TGS826 | Ammonia |
| TGS823 | Organic Solvent Vapors, Alcohol |
| TGS832 | Chlorofluorocarbons CFC's |
| TGS2600 | Air Contaminants, Hydrogen |
| TGS2612 | Methane and LP Gas |
| TGS2620 | Organic Solvent Vapors, Alcohol |
| TGS2602 | Air Contaminants, VOC, $H_2S$ |

Table 2: The target gases of the 8 MOS used in the wine case study

### *2. Sampling Approach*

Static headspace has been commonly used in e-nose applications dedicated to wines [9, 53, 54]. Similarly, the samples were placed in sealed bottles with a rubber septum. The built-in pump was equipped with a rubber tube ending with a syringe needle. The needle was used to pierce into the sealed bottles without comprising the medium or releasing the aerosols trapped inside the static headspace. The headspace collected was then drawn into the sensors' chamber and held during the sampling phase. The pump was calibrated to draw the optimal volume of headspace. To calibrate the pump flow rate or volume extract/time, an inverted graduated cylinder was placed in a water bath. The rubber tube from the e-nose was passed into the end of the inverted cylinder while making sure it's dry. The water level at rest was recorded. The pump was turned on for a defined short period of time. The water level increased, and the new level is noted. The flow rate of the pump is the difference between the two levels over the time the pump was turned on. In this setup it was found to be ~10 mL/sec empirically.

### *3. IoT E-Nose Configurations*

Parameters of the proposed e-nose were found after numerous empirical testing. Best performance was achieved with 8 sensors, a set-in time of 3 minutes and 0.5 seconds for sampling rate.

Concerning the sampling phase time: one momentary push button was configured to start the pump and to extract the sample aerosol from the sealed bottle

into the sensors' chamber. At the same time, the Micro Solenoid Valve is closed to trap the collected aerosol in the chamber. The pump then runs for 3 seconds to extract 30 mL of headspace volume. The phase will stay active for another 3 seconds to record the responses from the sensors in the chamber.

As for the cleaning phase time: one momentary push button was configured to start the pump to draw in fresh air and clear the sample aerosols from the sensors' chamber. At the same time, the Micro Solenoid Valve is opened to allow air to pass out of the sensors' chamber. An average of 6 minutes was required to bring the sensors back to stability.

**B. Tested Wines**

11 types of wines were selected from different sources. Subsets of each had matching features like color, winery, vintage, variety, or country, to reflect the different aspects that might affect the readings. The wines were selected to have similar alcohol content (12%-14%) to minimize the effect of alcohol on the classification. Each wine was given a unique identifier code. Table 3 summarizes the wines and their characteristics [55, 56].

| Name | Vintage | Color | Variety | Country | Winery/Source | Aroma/Taste Description from Source | Code |
|---|---|---|---|---|---|---|---|
| Chateau Ka Source de Rouge | 2013 | Red | Cabernet | Lebanon | Chateau KA | Spices, red fruits, peppery notes, and soft tannins | A |
| Massaya Le Colombier Red | 2016 | Red | Cabernet | Lebanon | Massaya | spice and pepper | B |
| Château Le Breton | 2016 | Red | Merlot | France | Bordeaux Supérieur | leather, minerals, cedarwood and ripe fruit | C |
| Arienzo | 2014 | Red | Tempranillo | Spain | Marqués de Riscal | Strawberries, red cherries, and toasted oak | D |
| Domaine de Mon Père | 2016 | Red | Grenache | France | Costières de Nîmes | violet and blackcurrant | E |
| Pinot Noir de Cana | 2013 | Red | Pinot Noir | Lebanon | Chatea Cana | ripe red cherry fruit, red berries and sweet spices | F |
| Cuvee St. Therese | 2016 | Red | Pinot Noir | Lebanon | Chateau Khoury | strawberry, spicy aromas, and intense tannins | G |
| Kefraya Blanc de Blancs | 2017 | White | Chardonnay | Lebanon | Chateau Kefraya | Muscat and floral notes, peach, watermelon, apricots, white flower, with honey and lilac | H |
| Reserve du Couvent | 2016 | Red | Cabernet | Lebanon | Chateau Ksara | wood and vanilla, and tannings | I |
| Ksara Blanc de Blancs | 2017 | White | Chardonnay | Lebanon | Chateau Ksara | floral aroma | J |
| Nuance by Chateau Ksara | 2017 | Rose | Malbec | Lebanon | Chateau Ksara | fruit aromas, melon, peach, pear | K |

Table 3: Different wines selected with varying and matching subsets of characteristics

## C. Procedure Applied

An empirical test was first performed using different volumes of wine. The known aerosol will provide a repeatable stable measurement that can be used to determine the best liquid to headspace volumes in the sealed bottles. After several trials with different volumes, a 50% liquid, 50% headspace ratio in the 60 ml sealed bottles gave the most stable responses with the least variations in repeated measurements. 5 samples, each of 30 ml, were taken from the same wine bottle immediately after opening and placed in 60 ml Thomas Scientific amber sample bottles with a pierceable

Teflon Silicon Septa in the cap. Total number of samples is 55 samples. 30 minutes were allocated for headspace equilibration after which measurements were done.

Each measurement was followed by a cleaning phase until sensors showed adequate stability. We repeated the process until all the samples were measured. To ensure the readings were not biased by drift or sensor poisoning of any kind, the order of readings of all samples was randomized.

**D. Live Data Visualization**

A crucial part of successful testing was monitoring the data through real-time visualization, to observe the sensors' behavior and perform any needed adjustments or corrections should they arise. For example, both in the set-in and cleaning phases of the e-nose work model, it is important to recognize when the sensors have stabilized as described earlier. An open source platform "Telemetry Viewer" [57] shown in Fig. 9, was used to visualize the received responses. An indicator has been added next to each sensor that would indicate if it was stable. A moving average window was used to calculate real-time averages of the sensors' response, with a configurable criterion to indicate if stability was reached. In this case study, if five consecutive averages of 20 consecutive points each exhibited less than 2% change, the sensors are reported as stable. The code was also slightly modified to add Bluetooth connectivity to receive data directly from the e-nose.

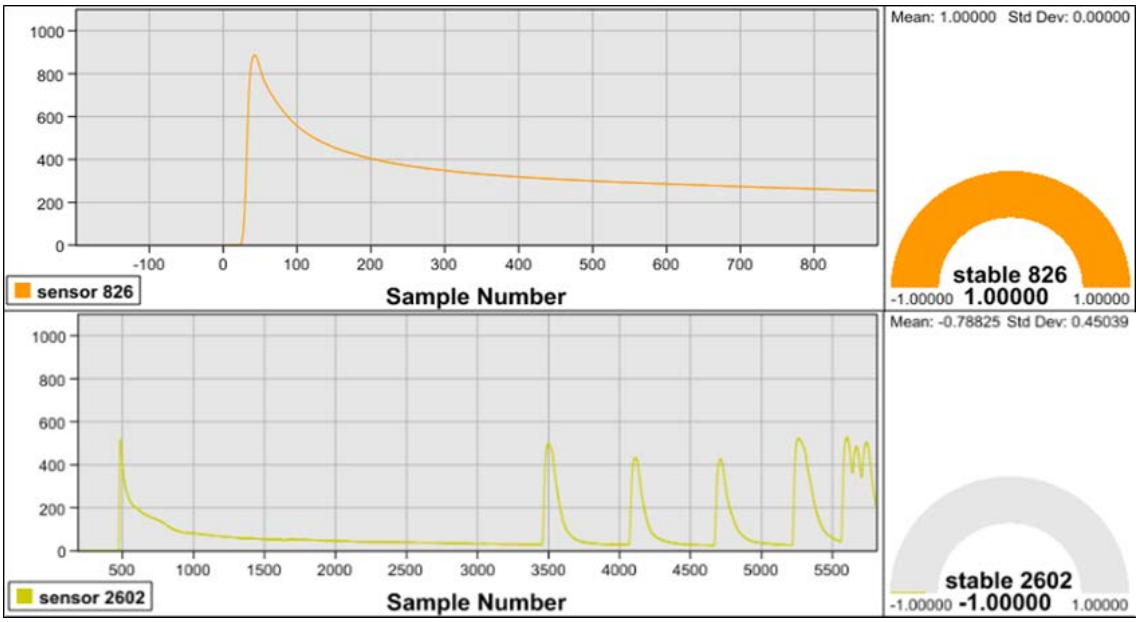


Fig. 9: Telemetry Viewer from [57] used to visualize the eight sensors response from the e-nose. The indicator on the side panel of each sensor shows if that sensor has achieved stability

# CHAPTER VII

# RESULTS

## A. Gathered Measurements

During the sampling phases, the sampling rate is 0.5 seconds; each measurement lasts until a stable response from the sensors is recorded. An average of 135 measurements or observations per sample was recorded, over 5 sample iterations for each wine, resulting in a total of 7453 observations. For each observation, 8 features were recorded corresponding to measurements from the 8 sensors.

## B. Result Profiles

A visual exploratory analysis was done first. The average of the steady state of each response curve for the 8 sensors was calculated. For example, the response for all samples were presented for wine B in a single radar plot to show repeatability of the measurements. As shown in Fig. 10, the contours for the radar plots for the different samples are closely overlapping, showing consistent response from all sensors.

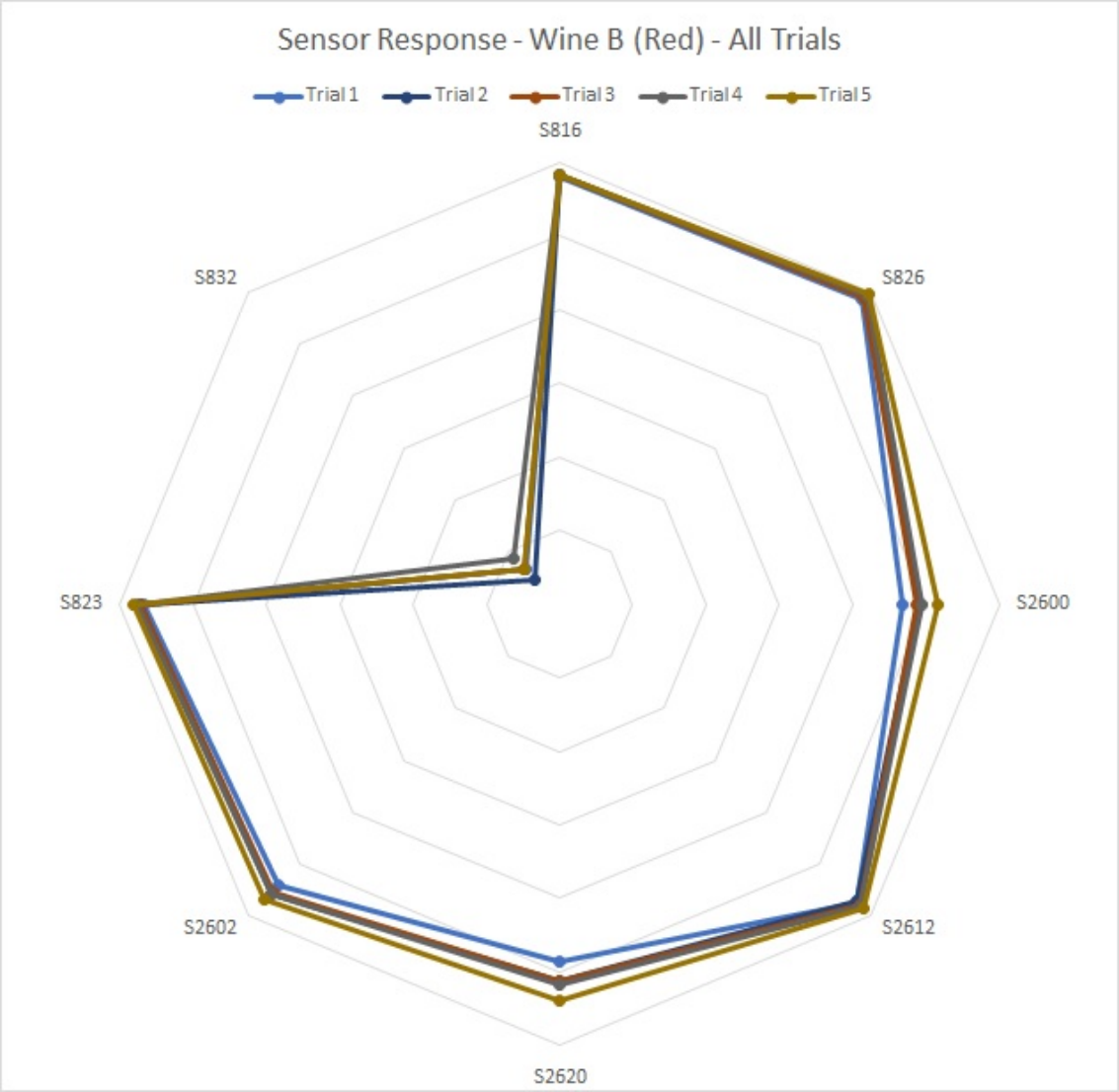


Fig. 10: Overlaid radar plots of the sensors' response of 5 samples taken from same wine type, wine B.

Next, the responses for a sample from different wine types were plotted in separate radar plots to show the discrimination capabilities of the e-nose. As shown in Fig. 11, the contour of the radar plots differs for different wine types. Fig. 12 displays

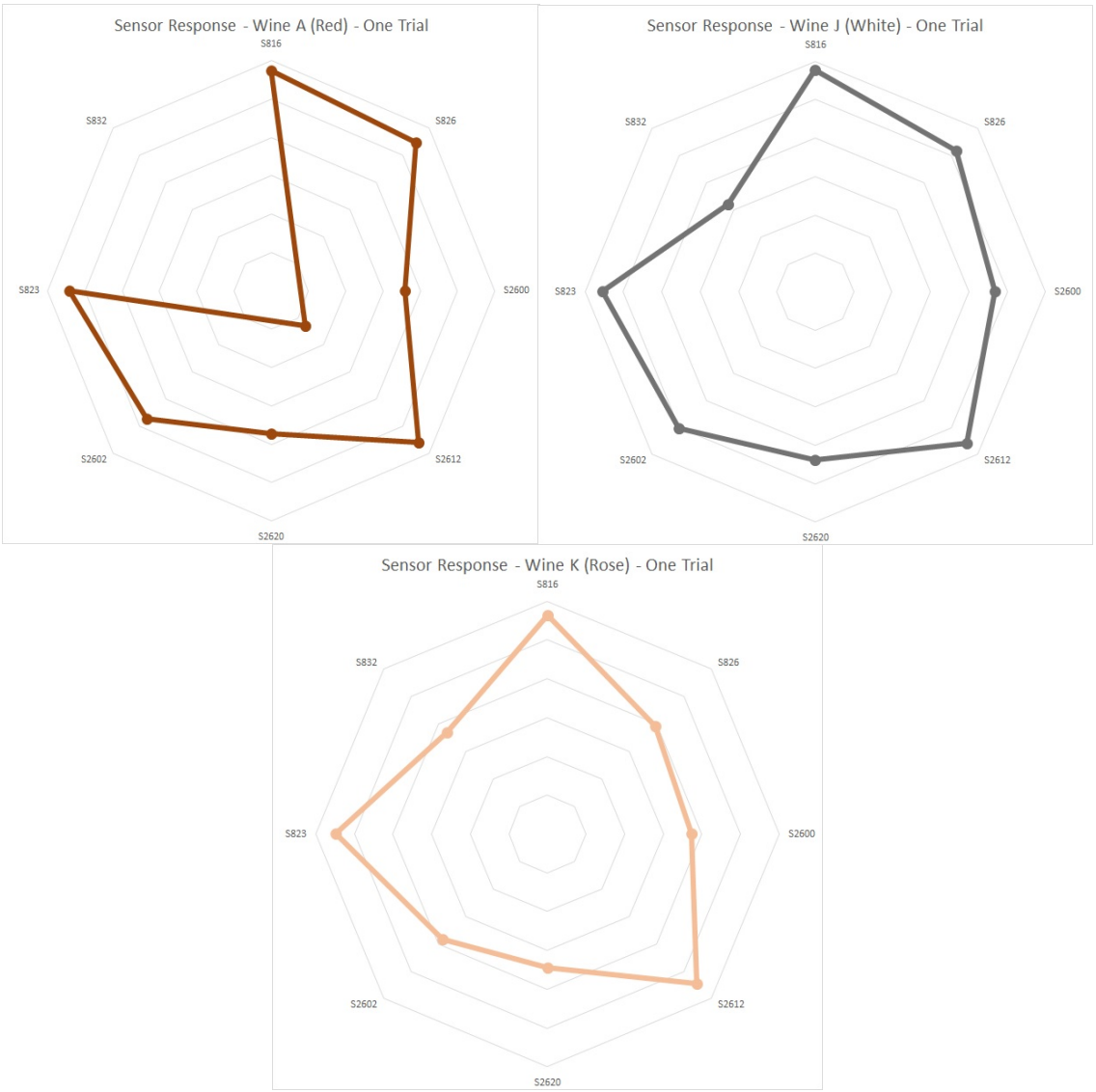


Fig. 11: Radar plots of the sensors' response to a sample from different wine types: wine A (red), wine J (white), wine K (rose).

the responses for a sample from each of the 11 wines used in the case study, overlaid in the same radar plot, highlighting the distinct sensor responses to the different generated odors.

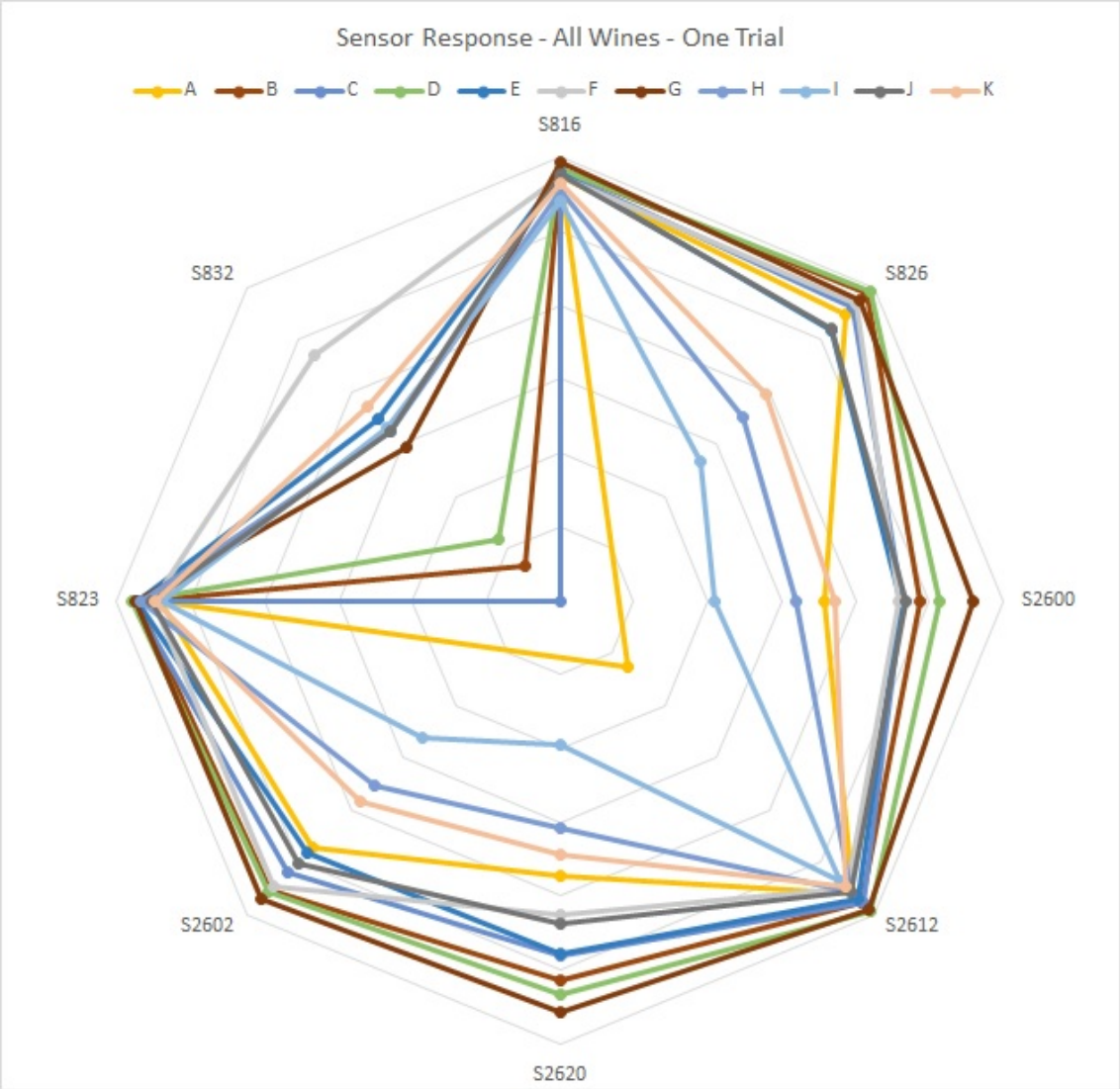


Fig. 12: Overlaid radar plots of the sensors' response for a sample from each of the 11 wines.

The visual representation of the sensors' response also gives insight into the sensors' role in odor discrimination between the different wine types. For example, S832, S2600, and S826 exhibited clear varying responses to each wine type. When we

plotted the response of each sensor (feature) versus another, a clear distinction between the wine types appeared, as shown in Fig. 13. The Arduino microcontroller has a 10-bit analog to digital converter. This means that it will map the input voltages received from the sensors which is between 0 and 5 volts into integer values between 0 and 1023. The corresponding values between 0 and 1023 as recorded by the Arduino microcontroller were used to plot the graphs below.

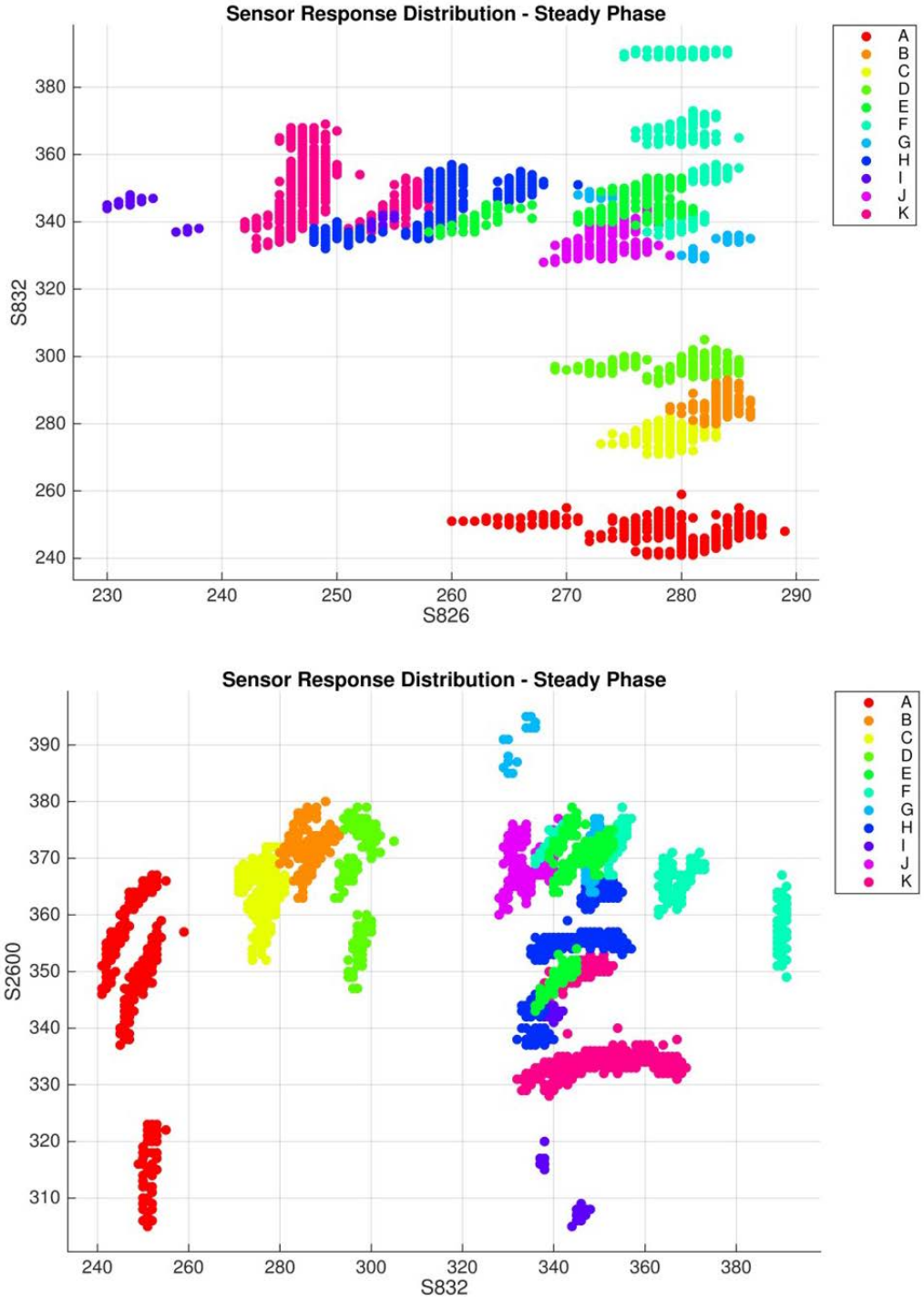


Fig. 13: Scatter plot of the response of different sensors. S826 vs S832 and S832 vs S2600 were plotted for all the observations in the steady-state. The observations for each wine type are color-coded to show the formation of clear clusters for each type.

## C. Classifications

In the following section we will highlight the results from the different pattern recognition algorithms used to train the classification model using different data subsets. The MOS used in our case study exhibit a signature response curve shown in Fig. 14. The response passes through a transient phase, where the value keeps increasing before reaching a stable plateau or steady-state [58]. Multiple approaches have been proposed for the characterization of response curves including maximum, average, slope, or steady state of each sensor [6, 28, 44].

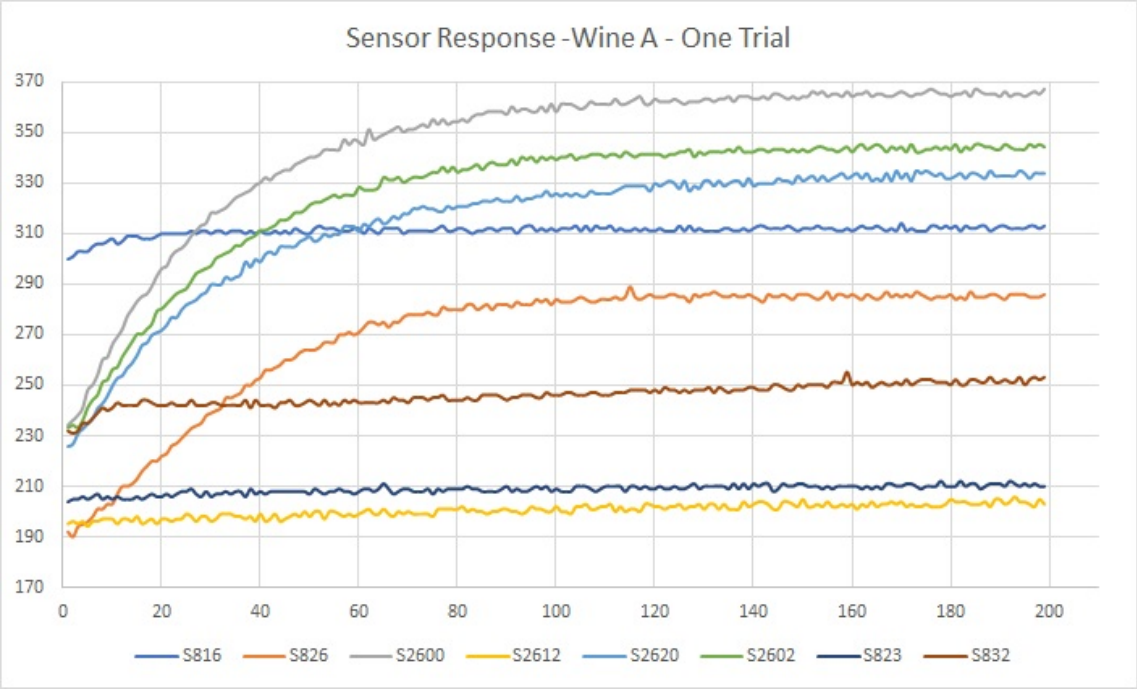


Fig. 14: Scatter plot of the sensors' response for a sample from wine A showing the signature response curve of MOS.

The steady state, which represents the maximum degree of reaction between the sensors and the aerosols, is often successfully used to characterize the sensors' response [24]. However, several studies have indicated that the transient response might have significant additional information that yield better prediction accuracy upon the classification using the steady-state alone [59]. Other studies found that transient phase response gave better classification results [60]. Another variation still was found with some studies, where using both transient and steady phase responses gave the best prediction model [61, 62]. Feature extraction from the sensor's response is a crucial point to train the models. As the jury is still not settled on which method would give the better performance, this paper will test the usage of each of the three datasets (transient, steady-state and combined) to construct the wine classification model [58].

A total of 7453 points were recorded as observations from the sensors to the different wine odors. The observations separated into 4361 points from the transient phase and 3092 points from the steady-state. The various sensors require different times to achieve stable state depending on the odors they are exposed to. The steady-state is only achieved when all sensors exhibit a stable response. The rough separation was performed using the stability indicator described earlier and through visual validation. Each observation has 8 features corresponding to the 8 sensors.

To train the different models, KNN, SVM, Decision Trees, and Artificial Neural Networks (ANN) learning algorithms were tested with varying parameters. For all data subsets used, the data was randomized and divided into training set and testing set. KNN, SVM, and Decision Trees were run with 10-fold cross-validation and varying

parameters. ANN was run with varying number of hidden layers, and neurons, with data distribution as 70% training set, 15% validation data, and 15% testing data. The top performing models generated from the above methods and using the three different dataset options is presented in Table 4 below.

| Phases | Decision Tree<br>Fine Tree, 100 maximum number of splits, Gini's diversity index | SVM<br>Cubic SVM, One-vs-One | KNN<br>Subspace KNN, nearest neighbors, 30 number of learners, 4 subspace dimension | ANN<br>2 hidden layers, 40 neurons each |
|---|---|---|---|---|
| **Steady State** | 98.2% | 99.3% | **99.8%** | 99.4% |
| **Transient State** | 83.9% | 96.5% | 93.0% | **98.1%** |
| **Combined** | 87.6% | **97.5%** | 94.9% | 97.5% |

Table 4: Prediction accuracy of the different algorithms applied to the transient, steady-state, and combined datasets

Using the transient phase data, ANN performed best with 98.1% prediction accuracy. Fig. 15 below shows the details of the confusion matrix. It is noted that misclassification occurred between Wine B as Wine C and vice versa. The two wines do not share common aroma/taste descriptors, but it is still possible that the chemical nature of their aromatic aerosols is close to each other and trigger the sensors in a similar manner leading to their misclassification. A similar behavior is seen between wines K and J although they exhibit different properties and flavor.

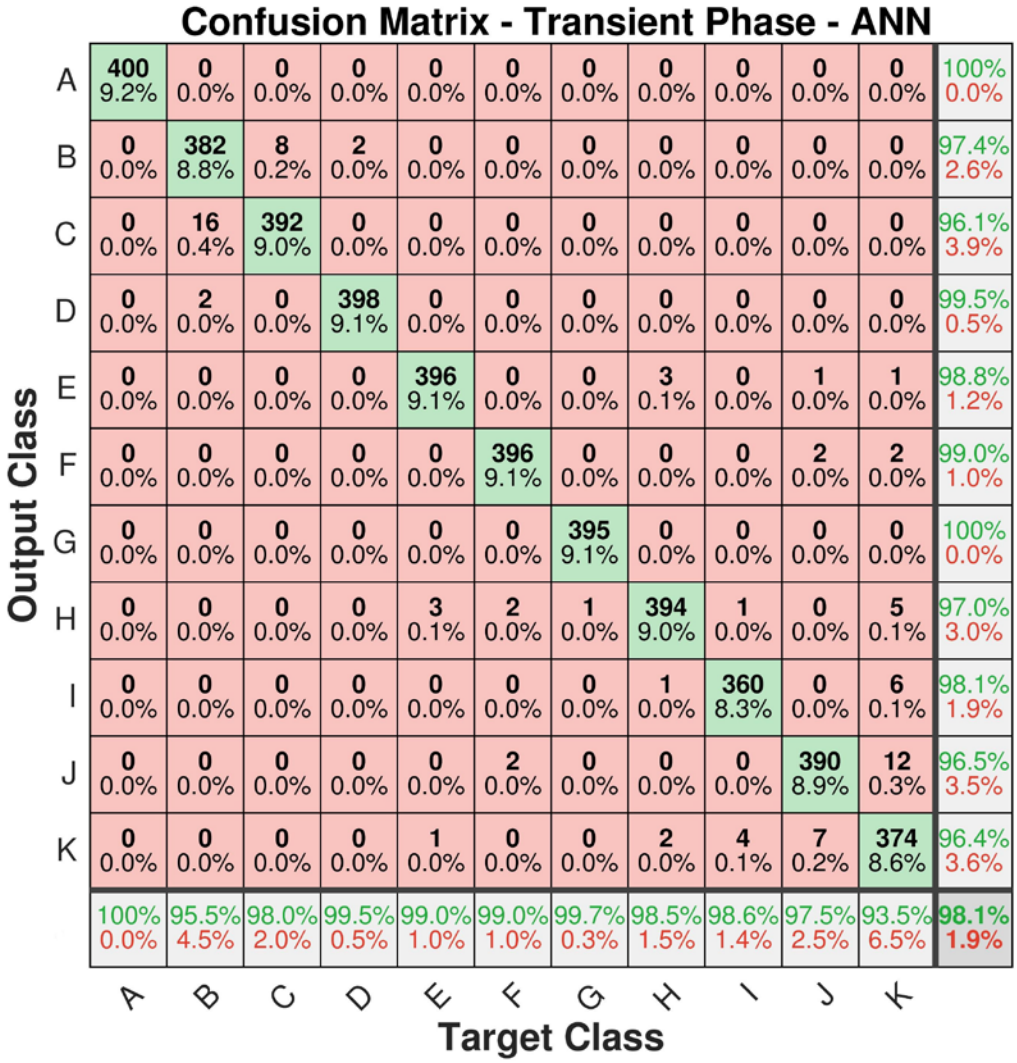


Fig. 15: Confusion Matrix of wine classification model trained with ANN algorithm using transient phase dataset.

Using the steady-state phase data, KNN performed best with 99.8% prediction accuracy. Fig. 16 below shows the details of the confusion matrix. Using the steady-state phase dataset gave the highest correct classification rate of all the other data sets. This was predicted from our radar plots which exhibited significant distinct unique pattern for each wine. Most wines yielded a 100% correct classification for most wines. We notice again a minor but mutual misclassification between Wine B and C where one is misidentified as the other.

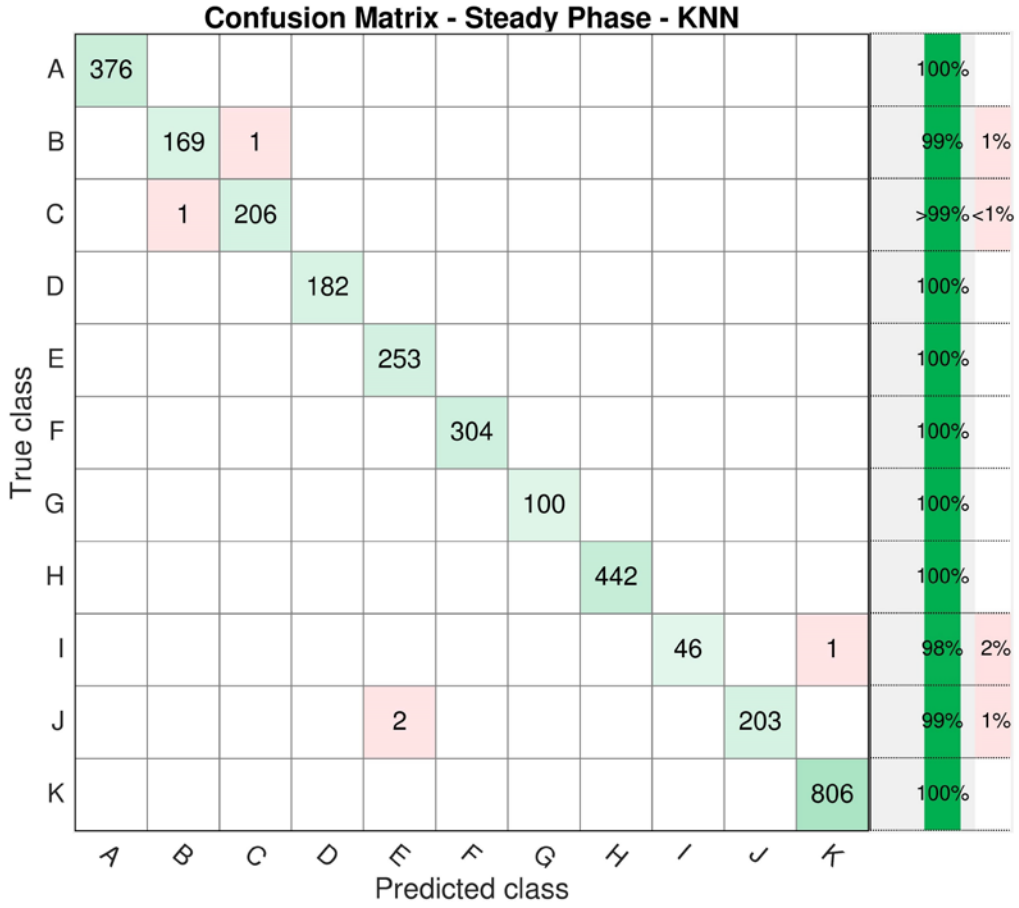


Fig. 16: Confusion Matrix of wine classification model trained with KNN algorithm using steady-state phase dataset.

Using the combined data from transient and steady-state phases, SVM performed best with 97.5% prediction accuracy. Fig. 17 below shows the details of the confusion matrix. The lowered accuracy rate is expected due to the varying nature of the responses from the sensors. However, it gives the most generalized model which encompasses the different stage of the e-nose response. We notice again the mutual misclassification of wine B and C. Other instances also arise between wine K and wine J, as well as wine K and wine I. The three wines are of different types, red, white and rose and don't share aroma descriptors as per descriptions from their source. However, it is noted that they are all from the same Winery, "Chateau Ksara". This might give some insight to similarity of aromatic aerosols exhibited by wines from the same orchid and region. Misclassification noticed between wine H and wine K can be attributed to their sharing of common aroma/taste descriptors like peach, watermelon and fruity notes. This behavior appears consistent throughout the wine types classification. It is more likely that misclassification occurs between wines with floral or fruity taste descriptors than those with spice, pepper or tannins descriptors.

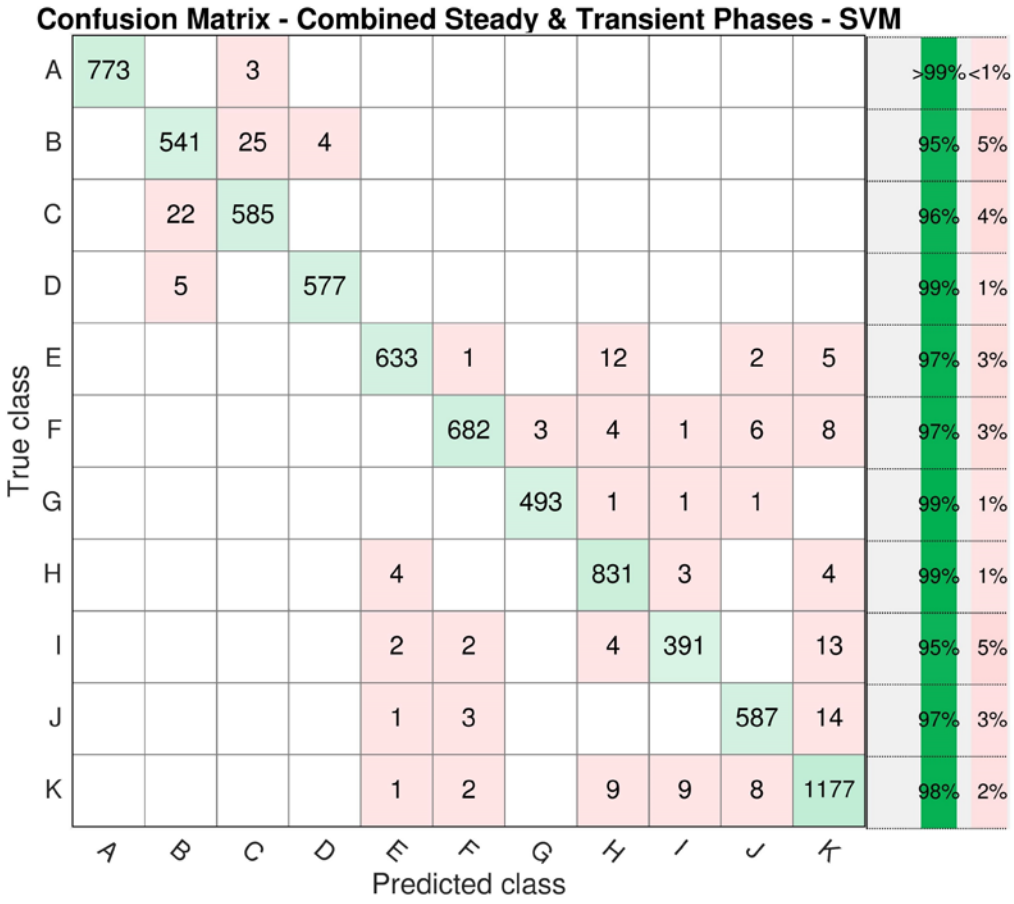


Fig. 17: Confusion Matrix of wine classification model trained with SVM algorithm using transient and steady-state dataset.

# CHAPTER VIII

# CONCLUSIONS AND FUTURE WORK

The introduction of sensors with higher sensitivity and smaller footprints, coupled with the increasing trend of IoT, hold promising potential for future work in enhancements and innovation in e-nose technology.

## A. Expansion of Circuitry

In future work on the suggested e-nose, we would give the circuitry a modular nature allowing expansions to support more sensors. One methodology is to set up the microcontroller and circuitry to communicate serially with similar electronic boards that can be added to them. This can allow different microcontrollers to control different types of sensors. Multiple e-noses used in literature have utilized novel sensors like coated quartz sensors and organic polymers, whose input can improve odor discrimination by multiple folds.

## B. Expansion of Enclosure

While typical e-noses rely on chemical interactions of the aerosols with the sensors to get a response, the mechanical aspect of the aerosols can offer valuable information and aid with odor discrimination which will be the subject of future work. One implementation called “TruffleBot” works as an extension to an e-nose [63]. It would add fluid mechanical and spatiotemporal dimensions to the data collected by the

typical e-nose through its own array of chemical, pressure, and temperature sensors in a small embedded platform. From tests performed, improvement in odor classification was detected.

### C. Software Support and Connectivity

Many experts predict the eventual spread of e-noses and connectivity to typical phones through Bluetooth. Future work will investigate the usage of everyday smart phones to perform odor tests of unknown samples against learned patterns from international databases, or to collect new data that can be uploaded to cloud-hosted aroma databases. By leveraging the power and spread of smart phones, it is possible to deploy software support for data collection, smoothing, analysis and testing on the go. Other communication modules like GPS might also introduce novel ways to use the e-nose. One suggestion would be using the e-nose to monitor pollution in real time while tracking location.

### D. Conclusions

A novel portable, versatile, low-cost, 3D-printed, IoT e-nose was presented, the advantages of which consist of its open source nature and ease of reproducibility and mass employability, for a cost of around $200. Cheap commercial MOS were used, powered by a common power bank battery. The components are commercially available, and the design can be readily manufactured in a standard university lab. The Arduino Microcontroller at its core allows for the customization behind the paper's

suggestion with basic electronics knowledge. The sensors can be interchanged to fit the targeted application. The e-nose is Bluetooth-connected, allowing for development of interfaces on any Bluetooth-ready device, thereby increasing its portability. The e-nose was tested in a wine classification exercise of ~7400 samples. A neural network algorithm was used, yielding a 99% prediction accuracy and showing the potential of the e-nose to become a useful unit in odor discrimination. As far as we know, no work offered an open source IoT e-nose for the scientific community and the masses. The outcome of making the technology accessible is a potential solution to its biggest problem of validation and reproducibility, giving way to constructing international databases and standardized data collection.

# REFERENCES


[1] R. Axel, "The molecular logic of smell," *Scientific American*, vol. 16, pp. 68-75, 2006.

[2] M. Anniko, M. Bernal-Sprekelsen, V. Bonkowsky, P. Bradley, and S. Iurato, *Otorhinolaryngology, Head and Neck Surgery*. Springer Science & Business Media, 2010.

[3] R. Axel, "The molecular logic of smell," *Scientific American*, vol. 273, no. 4, pp. 154-159, 1995.

[4] K.-T. Tang, S.-W. Chiu, C.-H. Pan, H.-Y. Hsieh, Y.-S. Liang, and S.-C. Liu, "Development of a portable electronic nose system for the detection and classification of fruity odors," *Sensors*, vol. 10, no. 10, pp. 9179-9193, 2010.

[5] B. M. Luke, R. SA, and S. MS. (2013). *ELECTRONIC NOSE (E-NOSE)*. Available: http://www.thetrinitycollege.wordpress.com/2013/07/15/electronic-nose-e-nose

[6] C. Cavanaugh, "An Adaptive Electronic Interface for Gas Sensors," Masters Thesis, North Carolina State University, 2002.

[7] S.-W. Chiu and K.-T. Tang, "Towards a chemiresistive sensor-integrated electronic nose: A review," *Sensors*, vol. 13, no. 10, pp. 14214-14247, 2013.

[8] J. Gonzalez-Jimenez, J. G. Monroy, and J. L. Blanco, "The Multi-Chamber Electronic Nose—An Improved Olfaction Sensor for Mobile Robotics," *Sensors*, vol. 11, no. 6, pp. 6145-6164, 2011.

[9] A. Loutfi, S. Coradeschi, G. K. Mani, P. Shankar, and J. B. B. Rayappan, "Electronic noses for food quality: A review," *Journal of Food Engineering*, vol. 144, pp. 103-111, 2015.

[10] H. R. Estakhroueiyeh and E. Rashedi, "Detecting moldy bread using an e-nose and the KNN classifier", *5th International Conference on Computer and Knowledge Engineering (ICCKE)*, pp. 251-255, 2015.

[11] K. Brudzewski, S. Osowski, and W. Pawlowski, "Metal oxide sensor arrays for detection of explosives at sub-parts-per million concentration levels by the differential electronic nose," *Sensors and Actuators B: Chemical*, vol. 161, no. 1, pp. 528-533, 2012.

[12] J. R. Askim, Z. Li, M. K. LaGasse, J. M. Rankin, and K. S. Suslick, "An optoelectronic nose for identification of explosives," *Chemical science*, vol. 7, no. 1, pp. 199-206, 2016.

[13] S. Chatterjee, M. Castro, and J.-F. Feller, "An e-nose made of carbon nanotube based quantum resistive sensors for the detection of eighteen polar/nonpolar VOC biomarkers of lung cancer," *Journal of Materials Chemistry B*, vol. 1, no. 36, pp. 4563-4575, 2013.

[14] M. Bruins, Z. Rahim, A. Bos, W. W. van de Sande, H. P. Endtz, and A. van Belkum, "Diagnosis of active tuberculosis by e-nose analysis of exhaled air," *Tuberculosis*, vol. 93, no. 2, pp. 232-238, 2013.

[15] E. Bales, N. Nikzad, N. Quick, C. Ziftci, K. Patrick, and W. Griswold, "Citisense: Mobile air quality sensing for individuals and communities design and deployment of the citisense mobile air-quality system," *6th International Conference on Pervasive Computing Technologies for Healthcare (PervasiveHealth)*, pp. 155-158, 2012.

[16] J. G. Monroy, J. Gonzalez-Jimenez, and C. Sanchez-Garrido, "Monitoring household garbage odors in urban areas through distribution maps," *SENSORS*, pp. 1364-1367, 2014.

[17] A. Somov, A. Baranov, D. Spirjakin, A. Spirjakin, V. Sleptsov, and R. Passerone, "Deployment and evaluation of a wireless sensor network for methane leak detection," *Sensors and Actuators A: Physical*, vol. 202, pp. 217-225, 2013.

[18] P. P. Neumann, V. H. Bennetts, A. J. Lilienthal, and M. Bartholmai, "From insects to micro air vehicles—A comparison of reactive plume tracking strategies," in *Intelligent Autonomous Systems 13*: Springer, 2016, pp. 1533-1548.

[19] J. Fonollosa, L. Fernandez, A. Gutiérrez-Gálvez, R. Huerta, and S. Marco, "Calibration transfer and drift counteraction in chemical sensor arrays using Direct Standardization," *Sensors and Actuators B: Chemical*, vol. 236, pp. 1044-1053, 2016.

[20] M. Khaydukova, D. Kirsanov, M. Pein-Hackelbusch, L. I. Immohr, V. Gilemkhanova, and A. Legin, "Critical view on drug dissolution in artificial saliva: A possible use of in-line e-tongue measurements," *European Journal of Pharmaceutical Sciences*, vol. 99, pp. 266-271, 2017.

[21] A. Perera, T. Sundic, A. Pardo, R. Gutierrez-Osuna, and S. Marco, "A portable electronic nose based on embedded PC technology and GNU/Linux: Hardware, software and applications," *Sensors Journal, IEEE*, vol. 2, no. 3, pp. 235-246, 2002.

[22] A. Gongora, J. Monroy, and J. Gonzalez-Jimenez, "An Electronic Architecture for Multipurpose Artificial Noses," *Journal of Sensors*, vol. 2018, 2018.

[23] R. Haddad, L. Carmel, N. Sobel, and D. Harel, "Predicting the receptive range of olfactory receptors," *PLoS computational biology*, vol. 4, no. 2, p. e18, 2008.

[24] N. El Barbri, E. Llobet, N. El Bari, X. Correig, and B. Bouchikhi, "Electronic nose based on metal oxide semiconductor sensors as an alternative technique for the spoilage classification of red meat," *Sensors*, vol. 8, no. 1, pp. 142-156, 2008.

[25] M. O'Connell, G. Valdora, G. Peltzer, and R. M. Negri, "A practical approach for fish freshness determinations using a portable electronic nose," *Sensors and Actuators B: chemical*, vol. 80, no. 2, pp. 149-154, 2001.

[26] M. C. C. Oliveros, J. L. P. Pavón, C. G. a. Pinto, M. E. F. Laespada, B. M. Cordero, and M. Forina, "Electronic nose based on metal oxide semiconductor sensors as a fast alternative for the detection of adulteration of virgin olive oils," *Analytica Chimica Acta*, vol. 459, no. 2, pp. 219-228, 2002.

[27] M. Pardo and G. Sberveglieri, "Coffee analysis with an electronic nose," *IEEE Transactions on Instrumentation and Measurement*, vol. 51, no. 6, pp. 1334-1339, 2002.

[28] M. M. Macías, J. E. Agudo, A. G. Manso, C. J. G. Orellana, H. M. G. Velasco, and R. G. Caballero, "A compact and low cost electronic nose for aroma detection," *Sensors*, vol. 13, no. 5, pp. 5528-5541, 2013.
[29] Z. Xie, "Electronic nose for analysis of volatile organic compounds in air and exhaled breath," 2017.
[30] J. Choi, J. S. Park, S. Chang, and H. R. Lee, "Multi-purpose connected electronic nose system for health screening and indoor air quality monitoring", *International Conference on Information Networking (ICOIN)*, pp. 495-499, 2017.
[31] R. Castro, M. K. Mandal, P. Ajemba, and M. A. Istihad, "An electronic nose for multimedia applications," *IEEE Transactions on Consumer Electronics*, vol. 49, no. 4, pp. 1431-1437, 2003.
[32] M. Iskandarani and N. Shilbayeh, "Design and analysis of a smart multi purpose electronic nose system," *Journal of Comp. Sc*, vol. 1, no. 1, pp. 63-71, 2005.
[33] The-eNose-Company. (2014). *eNose Technology*. Available: http://www.enose.nl/rd/technology/
[34] A. Berna, "Metal oxide sensors for electronic noses and their application to food analysis," *Sensors*, vol. 10, no. 4, pp. 3882-3910, 2010.
[35] A. D. Wilson, "Review of electronic-nose technologies and algorithms to detect hazardous chemicals in the environment," *Procedia Technology*, vol. 1, pp. 453-463, 2012.
[36] H. Singh *et al.*, "Metal oxide SAW E-nose employing PCA and ANN for the identification of binary mixture of DMMP and methanol," *Sensors and Actuators B: Chemical*, vol. 200, pp. 147-156, 2014.
[37] N. Barsan, D. Koziej, and U. Weimar, "Metal oxide-based gas sensor research: How to?," *Sensors and Actuators B: Chemical*, vol. 121, no. 1, pp. 18-35, 1/30/ 2007.
[38] E. J. Wolfrum, R. M. Meglen, D. Peterson, and J. Sluiter, "Metal oxide sensor arrays for the detection, differentiation, and quantification of volatile organic compounds at sub-parts-per-million concentration levels," *Sensors and Actuators B: Chemical*, vol. 115, no. 1, pp. 322-329, 5/23/ 2006.
[39] sparkfun.com. (2013). *Using the Arduino Pro Mini 3.3V*. Available: https://learn.sparkfun.com/tutorials/using-the-arduino-pro-mini-33v/all
[40] sparkfun.com. (2013). *Using the BlueSMiRF*. Available: https://learn.sparkfun.com/tutorials/using-the-bluesmirf#hardware-overview
[41] A. Wilson and M. Baietto, "Applications and advances in electronic-nose technologies," *Sensors*, vol. 9, no. 7, pp. 5099-5148, 2009.
[42] J. Lozano, J. Santos, J. Gutiérrez, and M. Horrillo, "Comparative study of sampling systems combined with gas sensors for wine discrimination," *Sensors and Actuators B: Chemical*, vol. 126, no. 2, pp. 616-623, 2007.
[43] J. P. Santos, J. Lozano, and M. Aleixandre, "Electronic Noses Applications in Beer Technology," in *Brewing Technology*: InTech, 2017.
[44] M. M. Macías, A. G. Manso, C. J. G. Orellana, H. M. G. Velasco, R. G. Caballero, and J. C. P. Chamizo, "Acetic acid detection threshold in synthetic

wine samples of a portable electronic nose," *Sensors,* vol. 13, no. 1, pp. 208-220, 2012.
[45] S. Capone *et al.*, "Aroma analysis by GC/MS and electronic nose dedicated to Negroamaro and Primitivo typical Italian Apulian wines," *Sensors and Actuators B: Chemical,* vol. 179, pp. 259-269, 2013.
[46] M. L. Rodríguez-Méndez *et al.*, "Electronic noses and tongues in wine industry," *Frontiers in bioengineering and biotechnology,* vol. 4, p. 81, 2016.
[47] G. Pioggia, M. Ferro, F. Di Francesco, A. Ahluwalia, and D. De Rossi, "Assessment of bioinspired models for pattern recognition in biomimetic systems," *Bioinspiration & biomimetics,* vol. 3, no. 1, p. 016004, 2008.
[48] L. Vera, M. Mestres, R. Boqué, O. Busto, and J. Guasch, "Use of synthetic wine for models transfer in wine analysis by HS-MS e-nose," *Sensors and Actuators B: Chemical,* vol. 143, no. 2, pp. 689-695, 2010.
[49] J. Lozano, J. P. Santos, M. Aleixandre, I. Sayago, J. Gutierrez, and M. C. Horrillo, "Identification of typical wine aromas by means of an electronic nose," *IEEE Sensors Journal,* vol. 6, no. 1, pp. 173-178, 2006.
[50] M. P. Martí, O. Busto, and J. Guasch, "Application of a headspace mass spectrometry system to the differentiation and classification of wines according to their origin, variety and ageing," *Journal of Chromatography A,* vol. 1057, no. 1-2, pp. 211-217, 2004.
[51] S. Buratti, S. Benedetti, M. Scampicchio, and E. Pangerod, "Characterization and classification of Italian Barbera wines by using an electronic nose and an amperometric electronic tongue," *Analytica Chimica Acta,* vol. 525, no. 1, pp. 133-139, 2004.
[52] Figaro. (2018). *Figaro Gas Sensors & Modules*. Available: http://www.figarosensor.com/product/sensor/
[53] D. Cozzolino, M. Holdstock, R. G. Dambergs, W. U. Cynkar, and P. A. Smith, "Mid infrared spectroscopy and multivariate analysis: a tool to discriminate between organic and non-organic wines grown in Australia," *Food Chemistry,* vol. 116, no. 3, pp. 761-765, 2009.
[54] M. Penza and G. Cassano, "Recognition of adulteration of Italian wines by thin-film multisensor array and artificial neural networks," *Analytica chimica acta,* vol. 509, no. 2, pp. 159-177, 2004.
[55] Enoteca. (2019). *Enoteca The House of Wine*. Available: https://www.enoteca.com.lb/products
[56] 209LebaneseWine. (2019). *209 Lebanese Wine*. Available: https://www.209lebanesewine.com/pages/lebanese-wineries
[57] F. Farahbod. (2017). *Telemetry Viewer*. Available: http://www.farrellf.com/TelemetryViewer/.
[58] J. Yan *et al.*, "Electronic nose feature extraction methods: A review," *Sensors,* vol. 15, no. 11, pp. 27804-27831, 2015.

[59] S. Roussel, G. Forsberg, V. Steinmetz, P. Grenier, and V. Bellon-Maurel, "Optimisation of electronic nose measurements. Part I: Methodology of output feature selection," *Journal of food engineering,* vol. 37, no. 2, pp. 207-222, 1998.

[60] E. Llobet, J. Brezmes, X. Vilanova, J. E. Sueiras, and X. Correig, "Qualitative and quantitative analysis of volatile organic compounds using transient and steady-state responses of a thick-film tin oxide gas sensor array," *Sensors and Actuators B: Chemical,* vol. 41, no. 1-3, pp. 13-21, 1997.

[61] S. M. Scott, D. James, and Z. Ali, "Data analysis for electronic nose systems," *Microchimica Acta,* vol. 156, no. 3-4, pp. 183-207, 2006.

[62] L. Carmel, S. Levy, D. Lancet, and D. Harel, "A feature extraction method for chemical sensors in electronic noses," *Sensors and Actuators B: Chemical,* vol. 93, no. 1-3, pp. 67-76, 2003.

[63] J. Webster, P. Shakya, E. Kennedy, M. Caplan, C. Rose, and J. K. Rosenstein, "TruffleBot: Low-Cost Multi-Parametric Machine Olfaction," in *2018 IEEE Biomedical Circuits and Systems Conference (BioCAS)*, 2018, pp. 1-4: IEEE.